

# Integrated MAP Equalization and Coding for Optical-Fiber-Communication Systems

Wenze Xi, *Member, IEEE*, and Tülay Adalı, *Senior Member, IEEE*

**Abstract**—In this paper, an integrated maximum a posteriori equalization and turbo product coding (IMAP-TPC) scheme for optical-fiber-communication systems (OFCS) is proposed. The scheme uses a probabilistic characterization of the electrical current in the presence of intersymbol interference (ISI) and noise to compensate their effects and improve the bit error rate. In the new IMAP-TPC scheme, TPC decoding is integrated with a symbol-by-symbol MAP detector. The MAP detector calculates the log-likelihood ratio of a received symbol using the conditional probability-density information and, hence, obtains a much more accurate reliability measure than the traditional measure used in the TPC decoder. The TPC was generated by serial concatenation of two Bose, Chaudhuri, and Hocquenghem codes with low overhead, which is a structure similar to a recently proposed hardware implementation of TPC decoder for optical systems. Simulation results with all-order polarization mode dispersion and amplified spontaneous emission noise demonstrate both the practicality and the effectiveness of the IMAP-TPC scheme for OFCS.

**Index Terms**—Forward error correction (FEC), integrated equalization and coding, maximum a posteriori (MAP) probability detection/equalization, probability-density-function (pdf) estimation.

## I. INTRODUCTION

**E**LECTRICAL-DOMAIN equalization techniques such as linear adaptive filters have been demonstrated to be effective in mitigating the effects of intersymbol interference (ISI) introduced by, e.g., the polarization mode dispersion (PMD) or chromatic dispersion in optical-communication systems [1]. These equalizers use a feedback or feedforward structure, and their coefficients are updated such that the mean square error (MSE) or another error statistic is minimized. Maximum-likelihood (ML) detection-based techniques, such as ML sequence (MLS) estimation (MLSE) or maximum a posteriori (MAP) detection, are recently proposed for PMD mitigation [2]–[4]. MLSE bases its decision on the observation of a sequence of received signals and searches for the best path through a trellis that maximizes the joint probability of the received signals. The MAP detector, on the other hand, makes decisions on a symbol-by-symbol basis and is optimum in the sense that it minimizes the probability of bit

errors. Both the MAP detector and the MLS estimator are superior to equalizers that rely on error metrics such as the MSE, as they directly minimize the errors in a symbol or sequence.

Amplified spontaneous emission (ASE) noise is the dominant noise source in optical-communication systems. At the end of optical-fiber propagation at receiver, the ASE noise generated by the amplifiers installed in the fiber accumulates and can significantly increase the bit error rate (BER). Forward error correction (FEC) coding has demonstrated to be an effective way to improve the reliability. It can be used to reduce the number of optical amplifiers used during optical-fiber transmission minimizing the required optical power and, hence, lowering the effects of fiber nonlinearity as well [11].

These two solutions, which are equalization and coding, are typically designed independent from each other. A scheme where the two are integrated and designed together, however, is much more desirable because of its potential to enhance the effectiveness of soft information interchange between the equalizer and the decoder. Moreover, the integration of equalization into decoding process does not increase the computational cost much, however, as we show in this paper, provides significant performance gains.

Joint coding and equalization (JCE) techniques [6] proposed for wireless or wireline communications systems is different from the integrated equalization and decoding technique proposed in this paper. JCE needs matched filters to generate the sufficient statistics [6], which is not available for optical-communication systems as these channels do not have the additive white Gaussian noise property. The propagation and the receiver structure in an optical-communication channel lead to nonlinear and non-Gaussian channel characteristics, and the photodetector that converts light into electrical current leads to a signal-dependent-noise term in the receiver. Our previous work [4] derives an analytical formula for the probability distribution of the filtered electrical current in the presence of the PMD and the ASE noise after the optical receiver and, hence, enables the design of such an integrated scheme for OFCS. In [15], we present a simple integrated equalization and coding scheme using a trellis-based ML decoding and note performance gains.

By building on the work in [4] and [16], in this paper, we develop an integrated MAP equalization and turbo product coding (IMAP-TPC) scheme. The design of TPC is based on a product of two constituent Bose, Chaudhuri, and Hocquenghem (BCH) codes using soft-input–soft-output (SISO) iterative decoding.

Manuscript received September 26, 2005; revised June 18, 2006. This work was supported by the National Science Foundation Award Number CCR-0123409.

The authors are with the Department of Computer Science and Electrical Engineering, University of Maryland, Baltimore County, Baltimore, MD 21250 USA (e-mail: wxi1@umbc.edu; adali@umbc.edu).

Digital Object Identifier 10.1109/JLT.2006.881482

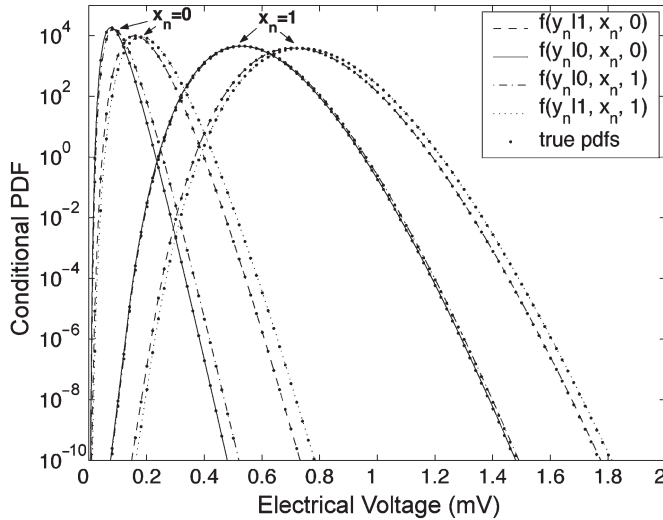


Fig. 1. Comparison between the estimated electrical conditional pdfs and the true pdfs denoted by solid dots where only 3-bit ISI is considered. The optical filter bandwidth is 80 GHz.

A suboptimal decoding algorithm—Chase-type II [14]—that can reach near ML decoding performance of linear block codes is implemented in an SISO iterative decoder to search for the most possible BCH codewords for soft decoding. The IMAP-TPC uses conditional probability density functions (pdfs) as the input of a symbol-by-symbol MAP detector, and integrates its output log-likelihood ratio (LLR) into soft decoder. Hence, it achieves a significantly better performance than the simple concatenated schemes and the integrated scheme we introduced in [15], where the conditional pdfs are integrated directly into the ML decoding process using the Viterbi algorithm. As we discuss in Section III, it is also different from turbo equalization as our approach offers a computationally and structurally simpler and more efficient technique for integrated equalization and coding.

We demonstrate the performance of a TPC with an overhead of 13.83%, which is practical for a 10-Gb/s OFCS implementation. Similar to the case in the experimental demonstration of TPC for OFCS built on a large-scale integrated circuit [11], we employ only a single iteration for practical considerations. Simulation results show a significant BER improvement using the IMAP-TPC scheme.

This paper is organized as follows. In Section II, we describe the general form of the MAP detector and MLSE for equalization with arbitrary memory length in the optical channel. In Sections III and IV, we introduce the integrated MAP equalization with TPC decoding and discuss its realization in a single-stage TPC decoder. Finally, in Section V, we present simulation results for the IMAP-TPC and compare its BER performance to the competing approaches.

## II. MLSE AND MAP DETECTION FOR OPTICAL-CHANNEL EQUALIZATION

A conditional electrical pdf, i.e., the distribution of the electrical current for a given transmitted sequence, provides

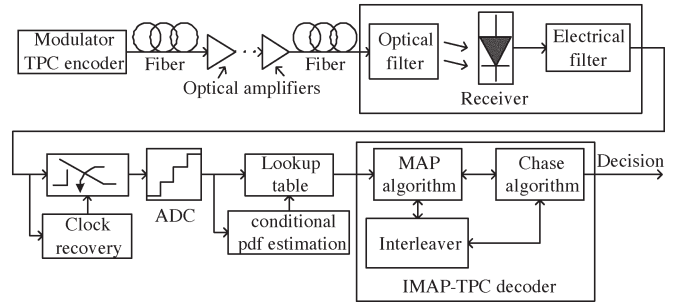


Fig. 2. Optical-communication system with integrated MAP equalization and TPC decoder.

the complete statistical information in the electrical domain for a channel with ISI and noise, provided it includes a memory to match the span of the ISI. An accurate characterization takes into account both the physical sources of ISI such as PMD and chromatic distortion and the effects of optical and electrical filters besides the distribution of noise. The conditional pdf, which describes the dependence of a received symbol on the transmitted bit sequence, has the form  $f_y(y_n | \dots, x_{n-2}, x_{n-1}, x_n, x_{n+1}, x_{n+2}, \dots)$ , where  $y_n$  denotes the sampled electrical current  $y(nt_0)$  in the  $n$ th bit slot after clock recovery, and  $x_n$  denotes the corresponding transmitted information bit. The conditional pdf can thus be used for ML-based ISI compensation, such as in MLSE or MAP detection.

In [4], we show that one can practically estimate the conditional pdf of the electrical current given a transmitted sequence in the presence of PMD-induced ISI and ASE noise and use these conditional pdfs to implement a symbol-by-symbol MAP detector and an MLS detector to compensate for the PMD-induced pulse spreading and distortion in the received signal. In Fig. 1, we compare the estimated conditional pdfs with the true pdfs of the electrical current. The true pdfs are calculated assuming that the optical phase is known before the receiver. However, the estimated pdfs are calculated using the mean electrical current value without any optical phase information. As we can see, the estimated conditional pdfs agree very well with the true pdfs. In other words, even without the knowledge of the optical phase, we can estimate the conditional pdfs fairly accurately. These pdfs, as we show in Section V, provide valuable information required for ML-based equalization and soft decoding. In the following development, we assume that the conditional pdfs are estimated such that the main sources of ISI and noise are taken into account. We also note that  $x_i \in \{0, 1\}$  and that the ISI-induced pulse spreading is contained within a window of length  $2j - 1$  bits, where  $j$  is an integer.

To detect the  $i$ th symbol such that  $i > j$ , the decision window  $[m, m + 2j - 2]$  of length  $2j - 1$  of a MAP detector is shifted over the received sequence, where  $m > 1$ . The decision is made by the evaluation of

$$\hat{x}_i = \arg \left\{ \max_{x_i} F(\mathbf{y}|x_i) \right\} \quad (1)$$

where  $\mathbf{y} = (y_i, y_{i+1}, \dots, y_{m+2j-1})$ , and

$$\begin{aligned}
 F(\mathbf{y}|x_i) &= \sum_{x_{i+1}, \dots, x_{m+2j-2}} f(y_i|x_m, x_{m+1}, \dots, x_{m+2j-2}) \\
 &\times \sum_{x_{m+2j-1}} f(y_{i+1}|x_{m+1}, x_{m+2}, \dots, x_{m+2j-1}) \dots \\
 &\times \sum_{x_{m+3j-2}} f(y_{m+2j-1}|x_i, \dots, x_{m+3j-2}). \quad (2)
 \end{aligned}$$

The MLS detector in the presence of both ISI and noise is given by [15]

$$\hat{\mathbf{x}} = \arg \left\{ \max_{\mathbf{x}} \prod_{i=m+j}^N f(y_i|x_m, x_{m+1}, \dots, x_{m+2j-2}) \right\} \quad (3)$$

where  $\mathbf{x} = (x_i, x_{i+1}, \dots, x_N)$ , and the Viterbi algorithm is used to determine the most likely sequence [12].

Both the MAP detector and the MLS estimator are optimum in the sense that they minimize the BER. MLS estimator bases its decision on a sequence of received signals and searches for the best path through a trellis to maximize the joint probability of the received signals. The trellis structure of the MLS estimator, however, introduces a significant time delay during decision. Moreover, as the memory length of the optical channel increases, the number of trellis states increases exponentially. The MAP detector, on the other hand, makes decisions on a symbol-by-symbol basis. It introduces a much smaller time delay during decision than an MLS estimator. The LLR of the received symbol can also be calculated by first finding  $\hat{\mathbf{x}}$  and its complementary symbol  $\hat{\mathbf{x}}_c$  using (1) and then comparing the LLR of  $x_i = \hat{\mathbf{x}}$  to  $x_i = \hat{\mathbf{x}}_c$  using (2). The received symbol LLR (the output of the MAP detector) provides not only the noise information but also the ISI information, e.g., which is introduced by PMD or chromatic dispersion. Hence, it can be integrated into soft decoding process in an FEC decoder, which is significantly to reduce the BER.

### III. INTEGRATED MAP EQUALIZATION AND TPC CODING

As described in the previous section, estimated conditional pdfs can be used for ML-based equalization techniques, such as MLSE and symbol-by-symbol MAP detection for dispersion compensation. Meanwhile, they can also be used for iterative SISO TPC decoding methods. In this paper, we propose an effective IMAP-TPC scheme (shown in Fig. 2) using the estimated conditional pdfs and the symbol-by-symbol MAP detection. The symbol-by-symbol MAP detector uses the given conditional pdf as its input and outputs the LLR soft information by observing a received sequence and, hence, provides an improved reliability measure as the input to the TPC soft decoder. Finally, we propose using a suboptimal decoder that offers a good compromise between decoding performance and complexity so that the solution is attractive for implementation in an OFCS.

The proposed IMAP-TPC scheme is different from not only the turbo equalization but also from ML-based JCE meth-

ods based on [6] (see, e.g., [5]). Turbo equalization, which iteratively performs equalization and decoding, can achieve significant performance gains when ISI is present. However, it needs to exchange information between the equalizer and the decoder, therefore, is both computationally complex and is complicated in structure [7]. The ML-based JCE method has its theoretical foundation given in [6]. It has an MLSE receiver structure consisting of a whitened matched filter followed by a Viterbi decoder for Gaussian channels with ISI. In optical-communication channels, however, we cannot directly use the general concept of the ML-based JCE. Due to the presence of square-law detection in the receiver for an optical-communication system, the output electrical current consists of three parts: signal-signal beat, signal-noise beat, and noise-noise beat. We cannot find a whitening filter in the electrical domain so that the filtered output noise after sampling is independent and identically distributed for a signal-dependent noise [8]. In the IMAP-TPC scheme, the conditional pdfs and MAP detector is integrated within the decoding process. Since conditional pdfs take into account both noise and ISI, the soft decoding and MAP equalization are jointly optimized to reduce the BER.

The IMAP-TPC scheme begins with the calculation of a reliability measure for each received symbol. For a Gaussian symmetric channel without ISI and the transmitted bits  $e_i \in \{-1, +1\}$ , the reliability measure of the received symbol  $y_i$  is defined as [14]

$$l(y_i|e_i) = \log \left[ \frac{f(y_i|e_i = +1)}{f(y_i|e_i = -1)} \right] = \frac{2}{\sigma^2} y_i \quad (4)$$

where  $f(y_i|e_i)$  is the Gaussian distributed conditional pdf, and by using (4), Gaussian channel's reliability measure can be established by using the amplitude of the received signal. To find a reliability measure for the dispersive optical-communication channel, however, we cannot use (4) for the reliability measure. To find a reliability measure for the optical-fiber channel, several points need to be emphasized. If a communications channel is memoryless, then the noise process affecting a given bit in the received word is independent of the noise affecting the other received bits. In an optical-communication system, due to the PMD and the chromatic dispersion, the optical-communication channel cannot be assumed to be memoryless. Moreover, due to the complicated interactions of square-law detection and the optical and the electrical filters' effects in the receiver, the noise distribution is no longer Gaussian but is a generalized chi-square distribution [9]. These two fundamental changes require that the TPC decoding algorithm, especially the calculation of the reliability measure for each received symbol, is modified accordingly.

Let the BCH codeword  $\mathbf{C}(n, k)$  be the constituent codeword of TPC, where  $n$  and  $k$  stand for the codeword length and the number of information bits, respectively. The transmitted and received BCH codeword can be defined as  $\mathbf{x} = (x_1, x_2, \dots, x_n)$ , and  $\mathbf{y} = (y_1, y_2, \dots, y_n)$ , respectively. We

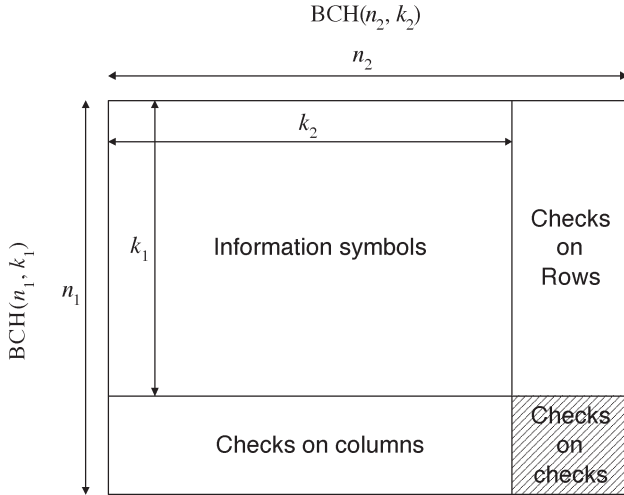


Fig. 3. Block diagram of  $BCH(n_1, k_1) \times BCH(n_2, k_2)$  product code.

calculate the reliability of a received symbol by finding the LLR value computed by a symbol-by-symbol MAP detector as

$$l_i = \log \frac{F(\mathbf{y}|x_i = 1)}{F(\mathbf{y}|x_i = 0)} \quad i = 1, 2, \dots, n \quad (5)$$

where  $F(\mathbf{y}|x_i)$  is defined by (2), and hence, combine equalization with the decoding process. Because the value  $l_i$  is the output LLR of the MAP detector, it contains information of both noise and ISI and, hence, provides an accurate reliability measure for use in TPC soft decoding.

For a practical IMAP-TPC implementation, we select a MAP detector integrated with two systematic linear block codes  $C_1$  and  $C_2$ , with parameters  $(n_1, k_1, d_1)$  and  $(n_2, k_2, d_2)$ , respectively. Here,  $n_i, k_i$ , and  $d_i$  ( $i = 1, 2$ ) stand for codeword length, number of information bits, and minimum Hamming distance, respectively. The product code  $P = C_1 \times C_2$  is obtained by

- 1) putting  $k_1 \times k_2$  information bits in a matrix with  $k_1$  rows and  $k_2$  columns;
- 2) coding the  $k_1$  rows using code  $C_1$ ;
- 3) coding the  $n_2$  columns using code  $C_2$ .

The resultant product code  $P(n', k', d')$ , as shown in Fig. 3, has parameters  $n' = n_1 * n_2$ ,  $k' = k_1 * k_2$ , and  $d' = d_1 * d_2$ . If  $t_1 = \lfloor (d_1 - 1)/2 \rfloor$  and  $t_2 = \lfloor (d_2 - 1)/2 \rfloor$  are the maximum random error correcting capability of the component codes  $C_1$  and  $C_2$ , respectively, the maximum random error correcting capability  $t'$  of the product code  $P$  is

$$t' = \lfloor (d - 1)/2 \rfloor = 2t_1t_2 + t_1 + t_2. \quad (6)$$

Because the decoding involves a two-step (rows after columns or vice versa) procedure, sometimes, it is incapable of correcting all the error patterns with  $t'$  or fewer errors in the code matrix  $P$  if these errors are beyond the BCH decoder's error-correction capability. However, such a decoding process is rather simple and efficient and, thus, practical. As we show later in the simulation section, it is quite effective as well. In the simulations, we choose  $n_1 = n_2 = 255$  and  $k_1 = k_2 = 239$  so that the TPC has a minimum distance of 25 and only 13.83%

overhead and, hence, is suitable for optical-fiber transmissions at 10 Gb/s or above [11].

The reliability measure of a received symbol is given by (5). However, to calculate the LLR of a received symbol in a BCH codeword  $C$  with codeword length  $n$  and information bit length  $k$ , one must take into account the fact that the ML codeword  $\hat{x}$  is one of the  $2^k$  codewords of  $C$ . By defining  $F(\mathbf{y}|\mathbf{x}) \equiv \prod_i^n F(y_i|x_i)$ , where  $\mathbf{x} = (x_1, x_2, \dots, x_n)$ ,  $\mathbf{y} = (y_1, y_2, y_3, \dots, y_n, y_{n+1}, \dots, y_{n+2l-2})$ ,  $\mathbf{y}_i = (y_i, y_{i+1}, y_{i+2}, \dots, y_{i+2l-2})$ , and  $2l + 1$  as the optical-channel memory length, we can write the LLR of a bit for different codewords  $C(n, k)$  as

$$l(x_i) = \log \frac{\sum_{\mathbf{x}^j \in S_i^1} F(\mathbf{y}|\mathbf{x} = \mathbf{x}^j)}{\sum_{\mathbf{x}^j \in S_i^0} F(\mathbf{y}|\mathbf{x} = \mathbf{x}^j)} \quad (7)$$

where  $S_i^1$  is the set containing the index of codewords  $\mathbf{x}^j$ ,  $j = 1, 2, \dots, 2^k$ , such that  $x_i^j = 1$ ,  $i = 1, 2, \dots, n$ , and  $S_i^0$  is the set containing the index of codewords  $\mathbf{x}^j$ ,  $j = 1, 2, \dots, 2^k$ , such that  $x_i^j = 0$ ,  $i = 1, 2, \dots, n$ .

Let  $C^1 \in S_i^1$  and  $C^0 \in S_i^0$  be the two most probable codewords, where  $C^1 = (c_1^1, c_2^1, \dots, c_n^1)$  and  $C^0 = (c_1^0, c_2^0, \dots, c_n^0)$ , and (7) can be rewritten as

$$\begin{aligned} l(x_i) &= \log \frac{F(\mathbf{y}|C^1)}{F(\mathbf{y}|C^0)} \\ &+ \log \left[ \frac{F(\mathbf{y}|C^0)}{F(\mathbf{y}|C^1)} \times \frac{\sum_{\mathbf{x}^j \in S_i^1} F(\mathbf{y}|\mathbf{x} = \mathbf{x}^j)}{\sum_{\mathbf{x}^j \in S_i^0} F(\mathbf{y}|\mathbf{x} = \mathbf{x}^j)} \right] \\ &= \log \frac{F(\mathbf{y}|C^1)}{F(\mathbf{y}|C^0)} \\ &+ \log \left[ \frac{1 + \sum_{\mathbf{x}^j \in S_i^1, \mathbf{x}^j \neq C^1} F(\mathbf{y}|C^0)F(\mathbf{y}|\mathbf{x} = \mathbf{x}^j)}{1 + \sum_{\mathbf{x}^j \in S_i^0, \mathbf{x}^j \neq C^0} F(\mathbf{y}|C^1)F(\mathbf{y}|\mathbf{x} = \mathbf{x}^j)} \right]. \end{aligned} \quad (8)$$

When the optical-communication channels operate with a high optical signal-to-noise ratio (OSNR), the second term of (8) is approximately zero, i.e.,  $\sum_{\mathbf{x}^j \in S_i^1, \mathbf{x}^j \neq C^1} F(\mathbf{y}|C^0)F(\mathbf{y}|\mathbf{x} = \mathbf{x}^j) \approx 0$  and  $\sum_{\mathbf{x}^j \in S_i^0, \mathbf{x}^j \neq C^0} F(\mathbf{y}|C^1)F(\mathbf{y}|\mathbf{x} = \mathbf{x}^j) \approx 0$ . By neglecting the second term in (8), an approximation for the LLR of decision  $x_i$  is obtained such that

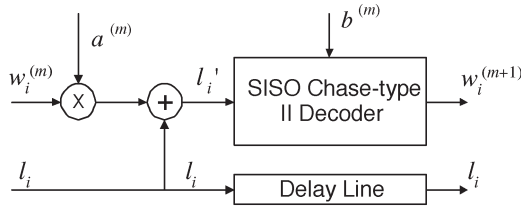
$$\hat{l}(x_i) = \log \frac{F(\mathbf{y}|C^1)}{F(\mathbf{y}|C^0)}. \quad (9)$$

By expanding (9), the following relation is obtained:

$$\hat{l}(x_i) = l_i + \sum_{j=1, j \neq i}^n l_j c_j^1 p_j \quad (10)$$

where

$$p_j = \begin{cases} 0, & \text{if } c_j^1 = c_j^0 \\ 1, & \text{if } c_j^1 \neq c_j^0 \end{cases}. \quad (11)$$


 Fig. 4. Block diagram of  $m$ th stage TPC decoder.

Defining  $w_i = \sum_{j=1, j \neq i}^n l_j c_j^1 p_j$ , (10) can be rewritten as

$$\hat{l}(x_i) = l_i + w_i. \quad (12)$$

In the next section, we describe how this quantity is used in the TPC decoder structure using the Chase algorithm [14].

#### IV. TURBO DECODING OF PRODUCT CODE

Fig. 4 shows the block diagram of the  $m$ th stage of a TPC decoder. The  $i$ th channel LLR value  $l_i$  is input to the delay line and added to the extrinsic information at the  $m$ th stage  $w_i^{(m)}$  to generate soft input  $l_i' = l_i + a^{(m)}w_i^{(m)}$ , where  $a^{(m)}$  is the  $m$ th stage scaling factor introduced to reduce the effect of extrinsic information when the BER is relatively high [13].

The LLR value  $l_i'$  is the input to the SISO Chase-type II decoder [14]. The Chase algorithm is a suboptimum procedure that uses a set of most likely error patterns. These error patterns are selected based on the reliability measure of the received symbols. Each pattern is added to the hard-decision received word and decoded using a hard-decision decoder. Each decoded codeword is scored by computing its joint probability with respect to the received (soft-decision) sequence. The codeword with the best joint probability is selected as the most likely.

The Chase decoder generates candidate constituent BCH codewords  $\{D_j\}$  using soft input  $l_i'$  and computes the LLR of transmitted symbol  $x_i$  within the set of BCH codewords such that

$$l_i'' = \log \frac{\sum_{D_j^1} F(\mathbf{y}|x_i)}{\sum_{D_j^0} F(\mathbf{y}|x_i)} \quad (13)$$

where  $D_j^1$  is the candidate codewords such that the  $i$ th bit is one, and  $D_j^0$  is the candidate codewords such that the  $i$ th bit is zero. Equation (9) can be used here to approximate (13). By subtracting  $l_i''$  from the soft input  $l_i'$ , we obtain output extrinsic information  $w_k^{(m+1)} = l_i'' - l_i'$  for the next decoding stage. If only one codeword is found, we can define a reliability measure  $b^{(m)}$ , as in [13], and calculate  $l_i'' = b^{(m)} s_j |l_i''|$ , where  $b^{(m)}$  is a positive number, and  $s_j \in \{-1, +1\}$  is the sign of the  $i$ th output LLR from BCH decoder.

#### V. APPLICATION OF IMAP-TPC TO PMD MITIGATION

In our simulations, we demonstrate the performance of IMAP-TPC scheme when applied to the PMD mitigation. We transmit bit sequences through a dispersive optical channel with all-order PMD and ASE noise. We use the conditional pdfs estimated (those shown in Fig. 1) and assume that the optical-

 TABLE I  
KEY PARAMETERS USED IN THE SIMULATIONS

parameter name	simulation values
data string length	65536
extinction ratio	20 dB
quantization bit	10
lookup table resolution	1024
pdf estimation resolution	1024

channel's memory length, i.e., the ISI, induced by all-order PMD is three, which means the conditional pdf conditioned on a three-bit sequence, i.e.,  $f_y(y_n|x_{n-1}, x_n, x_{n+1})$ .

Our numerical simulations are for a 10-Gb/s return-to-zero (RZ) transmission system using Gaussian pulses with a full width at half maximum (FWHM) of 50 ps, pulse rise time of 30 ps, and peak power of 1 mW. To include the effects of ISI due to the all-order PMD over a 1000-km fiber, we use the coarse-step method with 80 fiber sections for each 100-km optical signal transmission, as described in [10]. We did not impose any relationship between the principal states of the fiber and the input polarization state of the light. The ASE noise is added in the optical domain. After the fiber propagation and optical amplification, the distorted optical signal—in two polarization states—is filtered by a Gaussian optical filter with an FWHM bandwidth of 80 GHz and passes through a photodetector and a fifth-order electrical Bessel filter with a 3-dB bandwidth of 8 GHz. The electrical current is sampled and quantized after the clock recovery, and then, the estimated conditional pdfs shown in Fig. 1 are stored in a look-up table to be used in the IMAP-TPC method. The key parameters used in our simulations are given in Table I.

We implement  $\text{BCH}(255\ 239) \times \text{BCH}(255\ 239)$  product code with error-correction capability  $t = 2$  for each constituent BCH code. A rectangular interleaver with an interleaver depth of 255 is implemented between the row and column BCH encoder to generate the TPC code. Since the probability of PMD-induced ISI beyond the immediate neighboring bits due to a center bit in a sequence is very small, the memory length of optical fiber can be assumed to be three. Based on this assumption, we implement a three-symbol MAP detector to calculate the LLR of each symbol to be integrated into the SISO TPC decoder. In the TPC decoder, a Chase-type II SISO decoder is implemented. Instead of searching all possible codewords, as it is the case for ML decoding, Chase-type II algorithm only searches  $2^t - 1 = 3$  codewords. Error patterns are generated based on the unreliable positions of a received word using LLR from a MAP detector and then added to the received word to be decoded for BCH codewords. We implement Berlekamp–Massey algorithm [14] for the BCH hard decoder in the Chase-type II algorithm. Finally, the output LLR is calculated by (13), and extrinsic information is output for the next stage row/column decoding. Although the IMAP-TPC decoder can be used for iterative decoding, it is not practical in optical channels at data rates of 10 Gb/s and above. Additional iterations (feedback of soft information to the input of IMAP-TPC decoder) are computationally expensive, and multiple iterations are thus practically prohibitive. Thus, for practicality, we only use one iteration in our simulations.

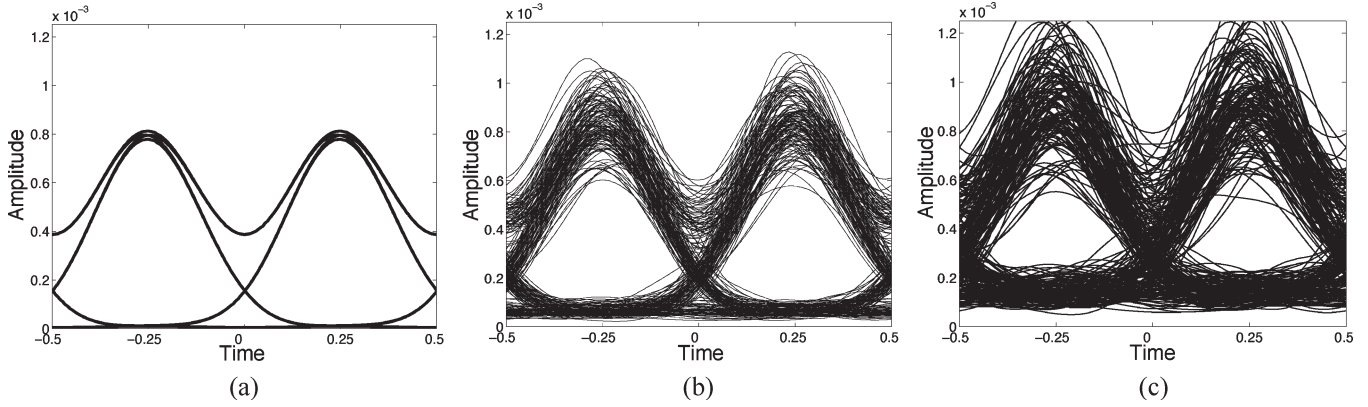


Fig. 5. Eye diagrams for DGD = 0 ps with different OSNRs. (a) Noise free, (b) OSNR = 12.23 dB, and (c) OSNR = 8.55 dB.

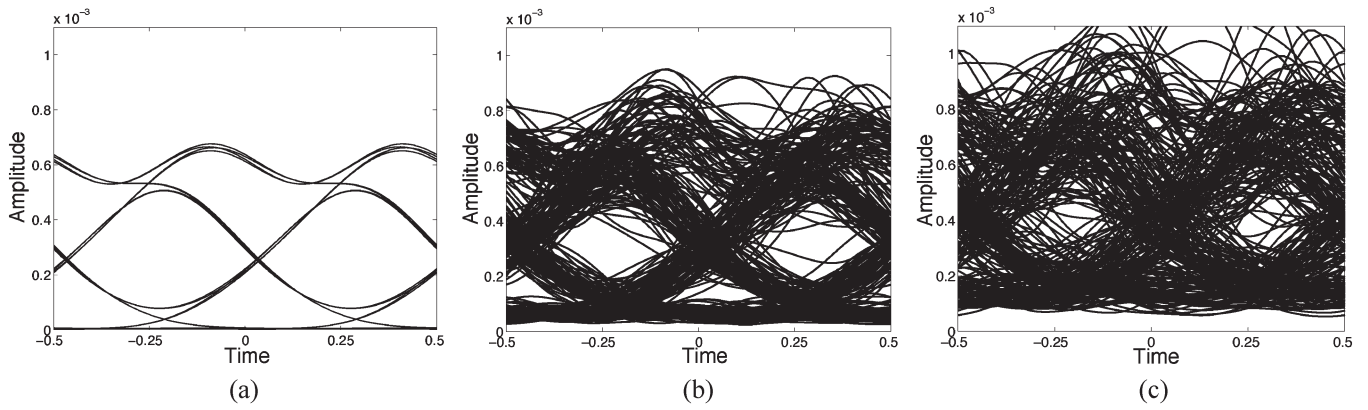


Fig. 6. Eye diagrams for DGD = 57 ps with different OSNRs. (a) Noise free, (b) OSNR = 12.23 dB, and (c) OSNR = 8.55 dB.

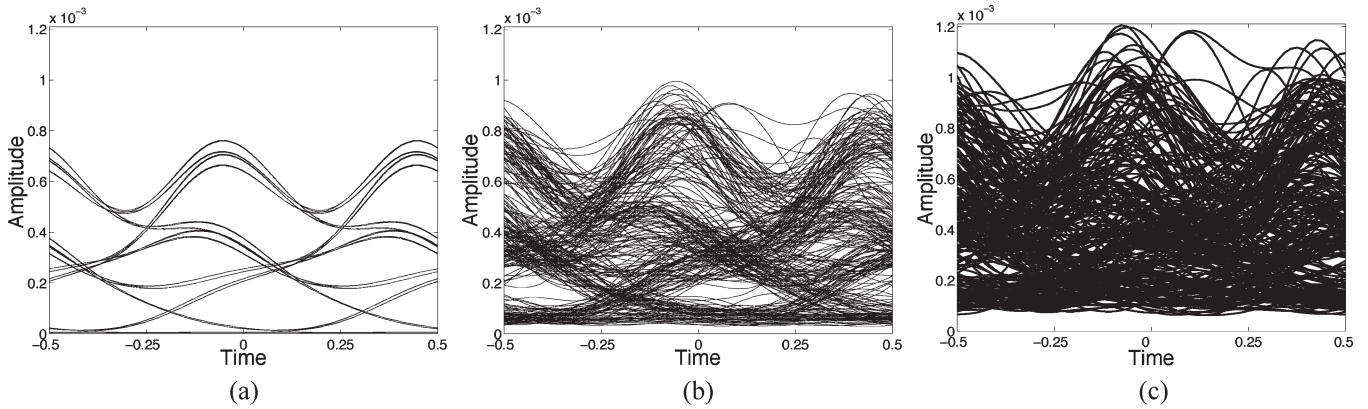


Fig. 7. Eye diagrams for DGD = 80 ps with different OSNRs. (a) Noise free, (b) OSNR = 12.23 dB, and (c) OSNR = 8.55 dB.

To evaluate the degree to which the IMAP-TPC compensates for the all-order PMD distortion and ASE noise in the optical fiber, we compare the BERs for the following cases: adaptive thresholding, MAP detector, and accurate conditional pdfs integrated with TPC. The TPC scheme uses conditional pdfs estimated, and hence, it is analogous to the TPC decoding process in binary unsymmetric channel with Gaussian distribution [11] but is more accurate in the pdf characterization it uses. We compare these four structures for different differential group delays (DGDs) and OSNRs. To illustrate the distortions

induced by different DGDs and degraded OSNRs, eye diagrams are given in Figs. 5–7. Fig. 5 compares the eye diagrams of a PMD-free signal (DGD = 0) with degraded eye patterns due to reduced OSNR. Figs. 6 and 7 show the eye diagrams for DGD = 57 ps and DGD = 80 ps with different OSNRs. The results shown in Figs. 8 and 9 are for a fixed fiber realization with a DGD of 57 and 80 ps, respectively. DGDs are chosen near the mean DGDs of fiber realizations. Although the BERs at 0.1–0.01 are not practical, they are added to the plots to demonstrate the overall trend of the BER.

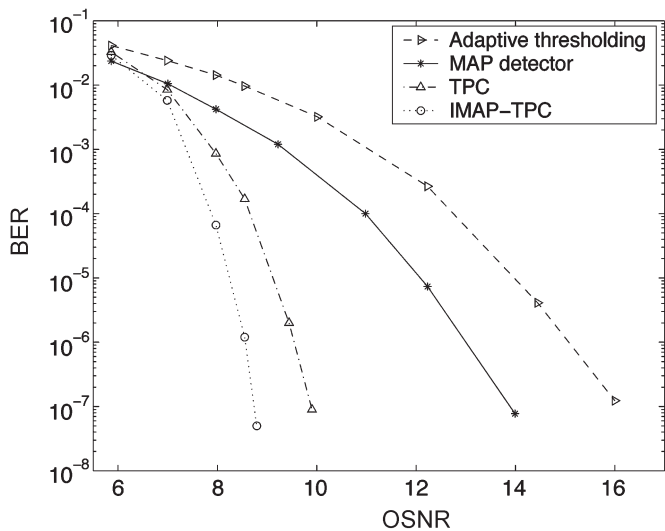


Fig. 8. BER versus OSNR comparison of four methods: Adaptive thresholding, MAP detector, TPC, and IMAP-TPC, where DGD is 57 ps.

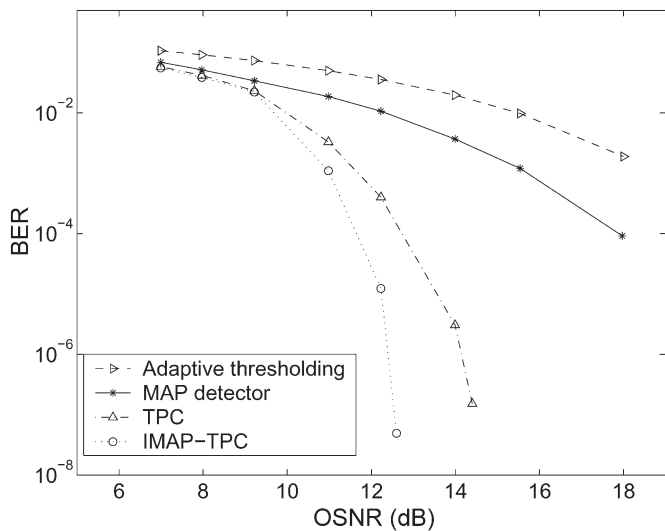


Fig. 9. BER versus OSNR comparison of four methods: Adaptive thresholding, MAP detector, TPC, and IMAP-TPC, where DGD is 80 ps.

As shown in Figs. 8 and 9, IMAP-TPC provides a significant improvement over the other methods as OSNR increases. In Fig. 8, when OSNR is 8.5 dB, the eye diagram in Fig. 6(c) shows an almost closed eye. However, IMAP-TPC provides almost two orders of magnitude gain with respect to TPC and more than three orders of magnitude gain for both methods of MAP detector and adaptive thresholding.

In Fig. 9, where DGD is large and the eye diagram shows a complete closed eye [Fig. 7(b) and (c)], IMAP-TPC still provides more than an order of magnitude gain with respect to TPC at OSNR 12 dB. In the large DGD case, the ISI produced by PMD will gradually spread beyond the immediate neighboring bits and, hence, violate the assumption that the ISI due to the center bit of a three-symbol sequence is well preserved in its neighboring bits. This is the main reason that we observe the BER saturation for MAP detector in Fig. 9. In this case, the conditional pdf needs to be estimated with larger

memory length, e.g., using a five- or seven-symbol sequence, and a MAP observation length increased accordingly. When there is no DGD, as expected, the IMAP-TPC performs just like the TPC. In this case, the MAP reliability measure calculated for the TPC decoding (IMAP-TPC) performs like a normal TPC decoder, because there is no intersymbol interference, and the input conditional pdfs for the MAP can only be conditioned on a symbol (a mark or a space) instead of a sequence of symbols, i.e., additional conditioning does not provide additional information.

We also notice that both TPC and IMAP-TPC do not perform very well in the low OSNR value. This is due to the large number of uncorrectable words during BCH decoding in Chase-type II decoder. As OSNR increases, especially to the point that word errors are within the error-correction capability of the BCH decoder, the system’s overall BER reduces drastically with the IMAP-TPC scheme.

### VI. CONCLUSION

We show how a MAP equalization can be integrated into a TPC decoder structure using electronically estimated conditional pdfs for significant performance gains. We demonstrate its application for the PMD mitigation in the presence of ASE noise by simulations.

It is worth reiterating that the use of IMAP-TPC is not limited to optical channels with PMD and ASE noise, but it is an effective solution for any source of ISI and noise, provided that an estimate of the conditional pdf is available. In our simulations, we calculated the conditional pdfs based on the method developed in [4], which provides an accurate conditional-pdf modeling and estimation in the presence of PMD and ASE noise. Development of techniques to efficiently estimate conditional pdfs in the presence of other distortion sources such as nonlinearity and chromatic dispersion will enable the use of the technique for compensation of a multitude of dispersion and noise sources.

To summarize, the IMAP-TPC scheme we introduced is both compact and practical in terms of its implementation for OFCS and can easily be integrated into a large-scale integrated circuit chip to enhance the system performance, making it promising for use in future short/long-haul OFCS.

### ACKNOWLEDGMENT

The authors would like to thank Dr. Cai for fruitful discussions, Dr. Zweck for fruitful discussions and assistance in the simulations, which are based on the Optical Communications Simulator (OCS), and Dr. Menyuk for fruitful discussions and the use of the Computational Photonics Laboratory computing cluster.

### REFERENCES

- [1] H. Bülow, “Electronic equalization of transmission impairments,” presented at the Optical Fiber Communication Conf. (OFC), Anaheim, CA, 2002, TuF.
- [2] T. Adali, “Signal processing for optical communications,” in *Proc. 15th LEOS*, Glasgow, U.K., 2002, vol. 2, pp. 623–624.

- [3] H. Bülow and G. Thielecke, "Electronic PMD mitigation—From linear equalization to maximum-likelihood detection," presented at the Optical Fiber Communication Conf. (OFC), Anaheim, CA, 2001, WAA3.
- [4] W. Xi, T. Adali, and J. Zweck, "A MAP equalizer for the optical communications channel," *J. Lightw. Technol.*, vol. 23, no. 12, pp. 3989–3996, Dec. 2005.
- [5] F. Xiong, "Sequential decoding of convolutional codes in channels with intersymbol interference," *IEEE Trans. Commun.*, vol. 43, no. 2, pp. 828–836, Apr. 1995.
- [6] G. D. Forney, "Maximum-likelihood sequence estimation of digital sequences in the presence of intersymbol interference," *IEEE Trans. Inf. Theory*, vol. IT-18, no. 3, pp. 363–378, May 1972.
- [7] R. Koetter, A. Singer, and M. Tüchler, "Turbo equalization," in *Proc. IEEE Signal Mag.*, Sep. 2003, pp. 67–80. Invited Paper.
- [8] O. Agazzi, D. Crivelli, and H. Carrer, "Maximum likelihood sequence estimation in the presence of chromatic and polarization mode dispersion in intensity modulation/direct detection optical channels," in *Proc. ICC*, 2004, vol. 5, pp. 2787–2793.
- [9] R. Holzlöhrner, V. S. Grigoryan, C. R. Menyuk, and W. L. Kath, "Accurate calculation of eye diagrams and bit error rates in optical transmission systems using linearization," *J. Lightw. Technol.*, vol. 20, no. 3, pp. 389–400, Mar. 2002.
- [10] D. Marcuse, C. R. Menyuk, and P. K. A. Wai, "Application of the Manakov-PMD equation to studies of signal propagation in optical fibers with randomly varying birefringence," *J. Lightw. Technol.*, vol. 15, no. 9, pp. 1735–1746, Sep. 1997.
- [11] T. Mizuochi, Y. Miyata, T. Kobayashi, K. Ouchi, K. Kuno, K. Kubo, K. Shimizu, H. Tagami, H. Yoshida, H. Fujita, M. Akita, and K. Motoshima, "Forward error correction based on block turbo code with 3-bit soft decision for 10-Gb/s optical communication systems," *J. Sel. Topics Quantum Electronics*, vol. 10, no. 2, pp. 376–386, Mar./Apr. 2004.
- [12] A. J. Viterbi, "Error bounds for convolutional codes and an asymptotically optimum decoding algorithm," *IEEE Trans. Inf. Theory*, vol. IT-13, no. 2, pp. 260–269, Apr. 1967.
- [13] R. M. Pyndiah, "Near-optimum decoding of product codes: Block turbo codes," *IEEE Trans. Commun.*, vol. 46, no. 8, pp. 1003–1010, Aug. 1998.
- [14] R. Morelos-Zaragoza, *The Art of Error Correcting Coding*. West Sussex, U.K.: Wiley, 2002.
- [15] W. Xi, T. Adali, and Y. Cai, "Probability distribution estimation for an integrated coding and equalization scheme in optical communications," in *Proc. ICASSP*, Philadelphia, PA, pp. iii/961–iii/964.
- [16] W. Xi and T. Adali, "Integrated MAP equalization and turbo product coding for optical fiber communications systems," Application No. 11/471, 717, Filed: Jun. 21, 2006.



**Wenze Xi** (S'01–M'06) received the B.Sc. degree (with honors) in communication engineering from Beijing Institute of Technology, Beijing, China, in 1997 and the Ph.D. degree in electrical engineering from the University of Maryland, Baltimore County (UMBC), in 2005.

From 1998 to 2000, he was a Wireless Network Engineer with Singapore Telecom. His research interests include adaptive signal processing, forward error correction (FEC), and their applications in optical-fiber communications.



**Tülay Adalı** (S'89–M'89–SM'98) received the B.S. degree from Middle East Technical University, Ankara, Turkey, in 1987 and the M.S. and Ph.D. degrees from North Carolina State University, Raleigh, in 1988 and 1992, respectively, all in electrical engineering.

In 1992, she joined the Department of Electrical Engineering, University of Maryland, Baltimore County, where she currently is a Professor. She worked on the organization of a number of international conferences and workshops, including the IEEE International Conference on Acoustics, Speech, and Signal Processing (ICASSP), the IEEE International Workshop on Neural Networks for Signal Processing (NNSP), and the IEEE International Workshops on Machine Learning for Signal Processing (MLSP). She was the General Co-chair for the NNSP workshops in 2001–2003 and the Technical Chair of the MLSP workshops in 2004–2006.

Dr. Adalı is the past Chair and current member of the MLSP Technical Committee and serves on the IEEE Publications Board and the IEEE Signal Processing Society conference board. She is an Associate Editor of the IEEE TRANSACTIONS ON SIGNAL PROCESSING and the *Journal of VLSI Signal Processing Systems*. Her research interests are in the areas of statistical signal processing, machine learning for signal processing, biomedical data analysis (functional MRI, MRI, positron emission tomography (PET), computed radiography (CR), ECG, and EEG), bioinformatics, and signal processing for optical communications. She is the recipient of a 1997 National Science Foundation CAREER Award.